

Assessment on the in-field lightpath QoT computation including connector loss uncertainties

Original

Assessment on the in-field lightpath QoT computation including connector loss uncertainties / Ferrari, Alessio; Balasubramanian, Karthikeyan; Filer, Mark; Yin, Yawei; Le Rouzic, Esther; Kundrát, Jan; Grammel, Gert; Galimberti, Gabriele; Curri, Vittorio. - In: JOURNAL OF OPTICAL COMMUNICATIONS AND NETWORKING. - ISSN 1943-0620. - ELETTRONICO. - 13:2(2021), pp. 156-164. [10.1364/JOCN.402969]

Availability:

This version is available at: 11583/2981094 since: 2023-09-11T15:27:18Z

Publisher:

OSA

Published

DOI:10.1364/JOCN.402969

Terms of use:

This article is made available under terms and conditions as specified in the corresponding bibliographic description in the repository

Publisher copyright

Optica Publishing Group (formely OSA) postprint/Author's Accepted Manuscript

“© 2021 Optica Publishing Group. One print or electronic copy may be made for personal use only. Systematic reproduction and distribution, duplication of any material in this paper for a fee or for commercial purposes, or modifications of the content of this paper are prohibited.”

(Article begins on next page)

Assessment on the in-field lightpath QoT computation including connector loss uncertainties

ALESSIO FERRARI^{1,*}, KARTHIKEYAN BALASUBRAMANIAN², MARK FILER², Yawei Yin², ESTHER LE ROUZIC³, JAN KUNDRÁT⁴, GERT GRAMMEL⁵, GABRIELE GALIMBERTI⁶, AND VITTORIO CURRI¹

¹DET, Politecnico di Torino, Corso Duca degli Abruzzi 24, Torino (TO), 10129, Italy

²Microsoft Corporation, Redmond, WA, USA

³Orange Labs, 22300 Lannion, France

⁴CESNET, Prague, Czech Republic

⁵Juniper Networks, Stuttgart, Germany

⁶Cisco Photonics, via S. M. Molgora, 48/C, Vimercate (MI), 20871, Italy

*Corresponding author: alessio.ferrari@polito.it

Compiled September 11, 2023

Reliable and conservative computation of quality of transmission (QoT) of transparent lightpaths (LPs) is a crucial need for software-defined control and management of the WDM optical transport. The LP QoT is summarized by the generalized SNR (GSNR) that can be computed by a QoT estimator (QoT-E). Within a context of network automation, the QoT-E must rely only on data from the network controller or provided by network elements through common control protocols and data structures. Therefore, given the theoretical accuracy of the QoT-E, the *in-field* accuracy in the GSNR computation is also determined by the level of knowledge of input parameters. Among these, a fundamental value is the connector loss at the input of each fiber span, that defines the actual power levels triggering the nonlinear effects in the fiber, and so defining the amount on nonlinear interference (NLI) and spectra tilt due to the stimulated Raman Scattering introduced by the fiber span. This value cannot be easily measured and may vary in time because of equipment update or maintenance.

In this article, we consider a lab measurement campaign in which the GSNR has been computed by means of the open source project GNPpy and analyze the computation error distribution. We show how the assumption on the value for the connector loss modifies the GSNR computation error, and show how the need for the GSNR computation to be accurate and conservative addresses toward lower values for connector loss. Using the outcome of the measurement campaign carried out in the lab, we present results in the error of GSNR computation in a production network. Specifically over two paths of the Microsoft core network. Using GNPpy with the assumption of connector loss of 0.25 dB as derived from the measurement campaign carried out in the lab, and using the physical layer description from the network controller, we show that GNPpy is not conservative by overestimating the GSNR only in 5% of cases, while in conservative predictions the underestimation error exceeds 1 dB only for few outliers. © 2023

Optical Society of America

<http://dx.doi.org/10.1364/ao.XX.XXXXXX>

1. INTRODUCTION

Networking technology is under fierce price pressure and the industry needs to adapt and drive structural changes. When big cloud providers faced a similar challenge of server hardware price pressure, they changed their business model by designing bespoke server platforms with standardized components. A similar trajectory is emerging for optical networks. So far,

the lack of standardization and agreed best practices in optical networking has not allowed operators to engage an open optical network approach, but standardization in optical networking is now ramping up, paving the way for network operators to design their own bespoke network.

It is notable that the push towards standardization comes at the crossroads of several trends in the industry. Coherent

technology and integrated optics allow the miniaturization of DWDM transceivers to an unprecedented level [1, 2] further enabling interoperability and standardization on component level. Equally, this trend is also pushing initiatives such as OpenConfig [3] and OpenROADM [4] aiming to disaggregate and standardize the optical network components. The other side of the coin is that operators embracing that new approach need to take on responsibility for the design and performance of their network rather than leaving it to system vendors. That move benefits from another trend: Software Defined Networking (SDN). SDN controllers enable fine grained control of networks through software, and operational logic previously bundled with optical equipment is disaggregated.

Early on, those trends have been identified by the Telecom Infra Project (TIP) open optical packet transport (OOPT) [5] working group which decided to create a physical simulation environment (PSE) working group to pioneer open optical network design and control. As a result, the Gaussian noise model in Python (GNPy) [6, 7] now provides operators access to the algorithmic foundation of planning and controlling optical networks [8]. It's currently targeting Operators rather than System vendors which means that a meticulous verification that GNPy is accurately predicting optical performance in deployed Operator Networks is a necessary step towards broader acceptance.

In past experiments, the quality of transmission estimator (QoT-E) of GNPy has been validated with excellent results with commercial equipment available in the lab [6, 9–11]. In these papers, the lack of knowledge on the connector losses is a key aspect for a quality of transmission (QoT) estimation, as mentioned in [11]. Therefore, in this paper we observe the impact of the connector loss uncertainty on the predictions of GNPy, showing that the value of 0.25 dB results to be the most conservative while accurate value. Then, we apply this strategy to compute the GSNR on two network segments of the Microsoft core network [12] by means of the GNPy's QoT, and we compare it to the measured GSNR. Such a comparison includes also aging factors such as sub-optimal connector cleanliness and in-line splices due to historical fiber cuts and repairs. This strategy proves its conservative capability keeping good accuracy since 95% of the errors are conservative and 90% of them are within ± 1 dB over a set of 114 measurements.

This paper is structured as follows: in Sec. 2 we describe the QoT-E of GNPy and the methodology adopted to get the network description needed by GNPy to compute the GSNR; then, in Sec. 3 we use the lab measurements to preform the analysis on the impact of the connector losses on the estimated QoT; in Sec. 4 we apply the outcomes of Sec. 3 on a deployed network and finally, in Sec. 5 we draw the final conclusions.

2. METHODOLOGY

A state-of-the-art optical network is a meshed network in which the LPs go through intermediate nodes transparently without being received and re-transmitted. For this reason, the physical layer must be approached considering the entire mesh network rather than isolating each point-to-point optical segment. In such a context the QoT is quantified by means of the generalized signal-to-noise ratio (GSNR) [10, 13]. Thus, the physical layer can be abstracted with a full disaggregated approach by means of a weighted graph whose nodes are the ROADM nodes and whose edges are the optical lines which are weighted by the corresponding GSNR contribution as shown in Fig. 1 [14]. Such

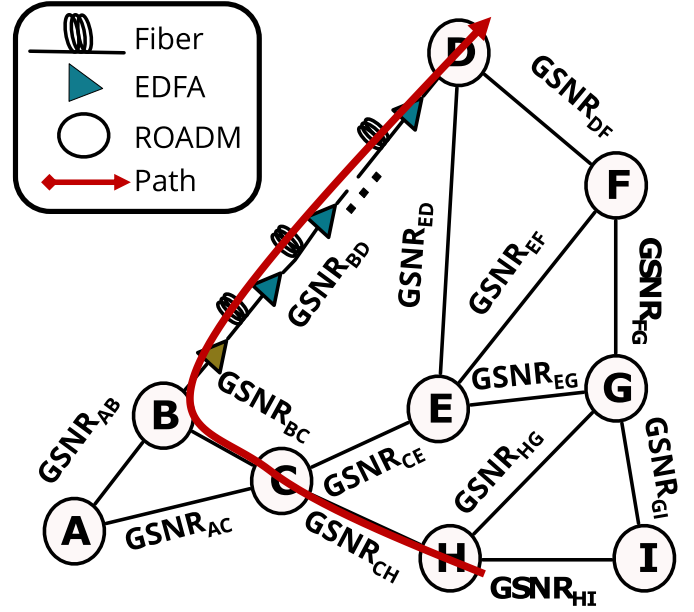


Fig. 1. Physical layer abstraction of an optical network.

GSNR contribution can be computed as

$$\text{GSNR}_{i,j} = \frac{P_s}{P_{\text{ASE}} + P_{\text{NLI}}}, \quad (1)$$

where, P_s is the signal power, P_{ASE} is the amplified spontaneous emission (ASE) noise power and P_{NLI} quantifies the NLI contribution of the link connecting the i -th node to the j -th node. Moreover, following a spectrally disaggregated approach, the NLI is comprised of self-phase modulation (SPM) and cross-phase modulation (XPM) terms, describing the self-channel interference (SC-NLI) of the channel on itself and the cross-channel interference (XC-NLI) caused by other channels, respectively. Moreover, the multi-channel interference is neglected as the contribution is very small for state-of-the-art optical networks as shown in [15]. Thus, the P_{NLI} of the n -th channel is evaluated as

$$\begin{aligned} P_{\text{NLI},n} &= P_{\text{SPM},n} + P_{\text{XPM},n} \\ &= \eta_{\text{SPM},n} P_n^3 + \sum_{m, m \neq n}^{N_{\text{ch}}} \eta_{\text{XPM},n,m} P_n P_m^2, \end{aligned} \quad (2)$$

where P_n is the power of the n -th channel at the input of the fiber, P_m is the input power of the m -th channel, η_{SPM} and $\eta_{\text{XPM},n}$ are the SPM efficiency and the XPM efficiency, respectively, and they depend on the symbol rate of the channels, the channel spacing, and the fiber characteristics. Each contribution has been evaluated by means of the generalized Gaussian noise (GGN) model [16–18].

The filter penalty introduced by the wavelength selective switches is negligible given the considered symbol rates and channel spacings.

The GSNR of a path (p) can be, therefore, evaluated by collecting the GSNR contribution of each link along the path as:

$$\text{GSNR} = \left(\sum_{(i,j) \in p} \text{GSNR}_{i,j}^{-1} \right)^{-1}. \quad (3)$$

GNPy is an open source software providing a QoT-E able to compute the GSNR of any path in an optical network. Such a

Table 1. Fiber parameters at 1550 nm.

Fiber type	α dB/km	D ps/nm/km	γ 1/W/km
SSMF	0.2	16.7	1.27
LEAF	0.222	3.8	1.45

module is the core of the GNPpy library, and it enables the use of GNPpy for network design and planning purposes, as a lighpath feasibility estimator in provisioning of lightpaths or to analyze the state of a network. Additionally, GNPpy provides a path computation module (PCM) that enables the development of an application program interface (API) for the integration with optical line system controllers [19–22].

In this article, we compare the GSNR measured from the transceiver cards with the one estimated with GNPpy. The GSNR computation by GNPpy was obtained by using information solely contained in the documentation of the network elements and measurements provided by the network equipment itself (such as the power values measured by the on-board photodiodes). Therefore, no dedicated characterization of the network or network elements was exploited. This is key to enabling the integration of GNPpy in a network automation framework where, a network controller automatically collects all the information by querying the network elements and a database storing the data written in the documentation and then it can provide the network description to the QoT-E and obtain the GSNR computation.

In order to estimate the GSNR it is necessary to provide to GNPpy relevant information on the ROADMs nodes, optical fibers, and amplifiers. More specifically, require the output power of the ROADMs nodes after the WSSes is retrieved by probing the booster amplifier. Then, the amplifiers' gain and tilt were provided by directly interrogating the amplifier configurations. Moreover, the amplifiers' NF were retrieved from the amplifier's documentation. Furthermore, knowledge of the fiber type and length (L_F) and the fiber type parameters are retrieved from the documentation related to the network. In presence of spans with Raman amplification, we retrieved the pump wavelength from the data-sheet and the pump power by querying the Raman card. The Raman solver evaluates both the Raman gain and the ASE noise introduced by the Raman amplifier.

To retrieve the actual GSNR, we measured the pre-forward error correction (FEC) bit-error-rate (BER) of each transceiver and then, we translated it into the corresponding GSNR by inverting the back-to-back (B2B) characteristic as described in [23]. Afterwards, the error has been evaluated as the measured GSNR minus the computed GSNR.

To observe the impact of the connector loss uncertainty, we provide to the QoT-E different reasonable values of connector losses: 0.25 dB, 0.5 dB and 0.75 dB. Therefore, we observe the error distribution in the three cases. Since the QoT computation must be conservative other than accurate, we use the value providing the larger number of conservative cases and we apply it to a measurement campaign carried out on two network segments of the Microsoft core network.

3. EXPERIMENT IN THE LAB

In this section we observe the impact of the connector loss on the errors by means of the measurement campaign carried out in

the lab experiment in the Microsoft lab [11]. Then, the outcome is used in the next section to make conservative while accurate assumptions on the connector losses.

A. Test-bed description

The test-bed depicted in Fig. 2 emulates a commercial network and it has six ROADMs nodes, five links and the longest path in the network is 2000 km. The transponders comes from three different vendors (Vendor A, B and C), while the line system comes from a fourth vendor (Vendor D).

Each ROADMs node is equipped with a booster and pre-amplifier per node degree. Each link is ~ 400 km long and makes use of four in-line amplifiers (ILA): three erbium-doped fiber amplifiers (EDFA) and one hybrid Raman-EDFA amplifier. The fiber types are ITU-T G.652 [24] standard single mode fiber (SSMF) and LEAF fiber and the fiber length varies from 65 km to 120 km. The fiber parameters are reported in Table 1. The exact location of each amplifier type and each fiber type and the fiber length of each span are shown in Fig. 2. Each amplifier and ROADMs have been configured for optimal performance by a vendor proprietary controller.

The transmitted WDM spectrum has a bandwidth occupation of 4.7 THz, from 191.3 THz to 196 THz. Commercial transponders from three different vendors are used to generate 26 channels grouped into five media-channels (MC): three MCs made of six channels and two MCs made of four channels. The WDM grid spacing is 50 GHz and the MCs are distributed as follows: two MCs are at the edges of the spectrum, a third MC is in the middle of the spectrum and the remaining two MCs are in the midpoints between the central MC and the external MCs. The rest of the spectrum has been filled with ASE noise to reach the full spectral load as shown in [25]. The signals are root-raised cosine shaped with a symbol rate of 34.16 GBaud and the roll-off is 0.2. All the transponders support PM-QPSK, PM-8QAM and PM-16QAM.

The state of the network was probed by querying the Microsoft software defined network (SDN) line system monitoring tool which is based on representational state transfer (REST) [26] in order to collect the needed data as described in Sec. 2.

In this test-bed, we measured several combinations of modulation format and distances: PM-QPSK at 2000 km and 4000 km, PM-8QAM at 400 km, 800 km, 1200 km, 1600 km and 2000 km and PM-16QAM at 400 km, 800 km and 1200 km, both in forward and in reverse directions. Since the longest bidirectional path in the line system is 2000 km, the 4000 km path was obtained by looping back the signals over the 2000 km path. Moreover, we also tested the 2000 km path with PM-8QAM without Raman amplification. This was achieved by turning off the Raman amplifiers and adjusting the EDFA gain to compensate for the absence of Raman gain.

B. Results

The error is computed as the difference between the measured and the estimated GSNR. Thus, positive errors are conservative as the GSNR estimate is smaller than the actual one, meaning that the impairments are overestimated. Likewise, negative error are non-conservative.

The tables 2 and 3 report the impact on the assumption of the connector loss on the percentage of conservative errors grouped by distance (table 2) and by modulation format (table 3). In general, by varying the distance, the number of conservative estimates always increases from $\sim 60\%$ up to 100%. The only exception is the case at 4000 km when the connector loss is 0.75 dB.

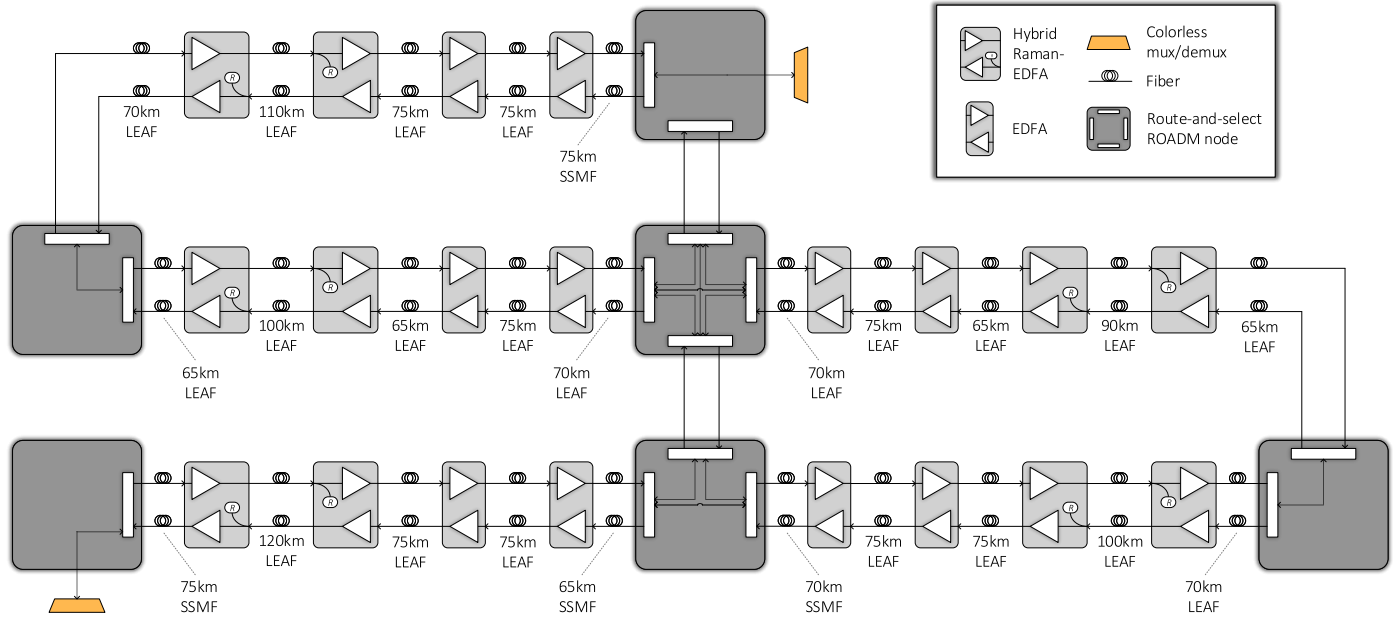


Fig. 2. The block scheme of the test-bed in the Microsoft lab.

Connector loss	400 km	800 km	1200 km	1600 km	2000 km	4000 km
0.25 dB	66%	75%	95%	98%	95%	100%
0.5 dB	60%	64%	86%	97%	90%	92%
0.75 dB	53%	57%	71%	89%	84%	77%

Table 2. The percentage of conservative errors for every distance.

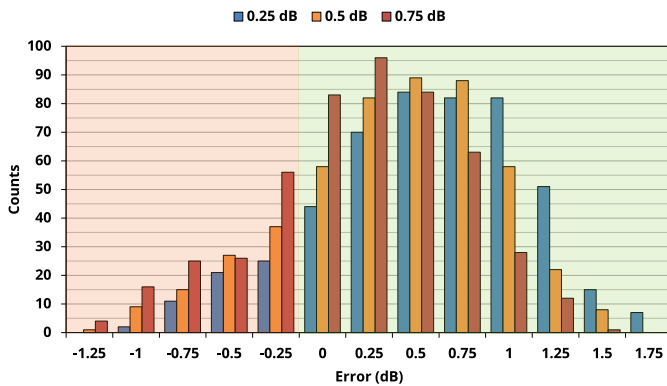


Fig. 3. Aggregated error distribution with different connector losses: 0.25 dB, 0.5 dB and 0.75 dB.

Connector loss	PM-QPSK	PM-8QAM	PM-16QAM
0.25 dB	97%	88%	78%
0.5 dB	86%	82%	69%
0.75 dB	68%	74%	63%

Table 3. The percentage of conservative errors for every modulation format.

Moreover, observing the modulation format, the quantity of positive errors is larger for the PM-QPSK and then, it decreases for PM-8QAM and it is minimum for the PM-16QAM. This is due to the fact that the PM-QAM has been observed at long distances (2000 km and 4000 km), i.e. where the estimates are more conservative, while the PM-8QAM has been observed between 400 km and 2000 km. Furthermore, the PM-16QAM has been observed between between 400 km and 1200 km. Finally, the trend on the conservative estimates increases by reducing the connector losses.

Fig. 3 shows the aggregated error distributions over more than 500 samples assuming a connector loss of 0.25 dB (blue bars), 0.5 dB (orange bars) and 0.75 dB (red bars). Moreover, the background of the histogram is red where the error is negative and thus, non conservative, while the background is green for the conservative cases. In all the cases the distribution is almost symmetric and all of them have a variance of ~ 0.5 dB, while the maximum error is ~ 1.75 dB for the connector losses equal to 0.25 dB, and ~ 1.5 dB for 0.5 dB and 0.75 dB. Moreover, the 88% of the errors are conservative when the connector loss is 0.25 dB. This quantity decreases to 82% when the loss is 0.5 dB and, finally it is 75% when the loss goes to 0.75 dB. This is reasonably due to the fact that a small connector loss leads to a larger power at the beginning of the fiber and thus an enhancement on the NLI. Therefore, it is possible to trade off the probability of having a non conservative estimation and the under-utilization of the available capacity. Since the conservatives is necessary to protect the communications from out of services, we choose a connector

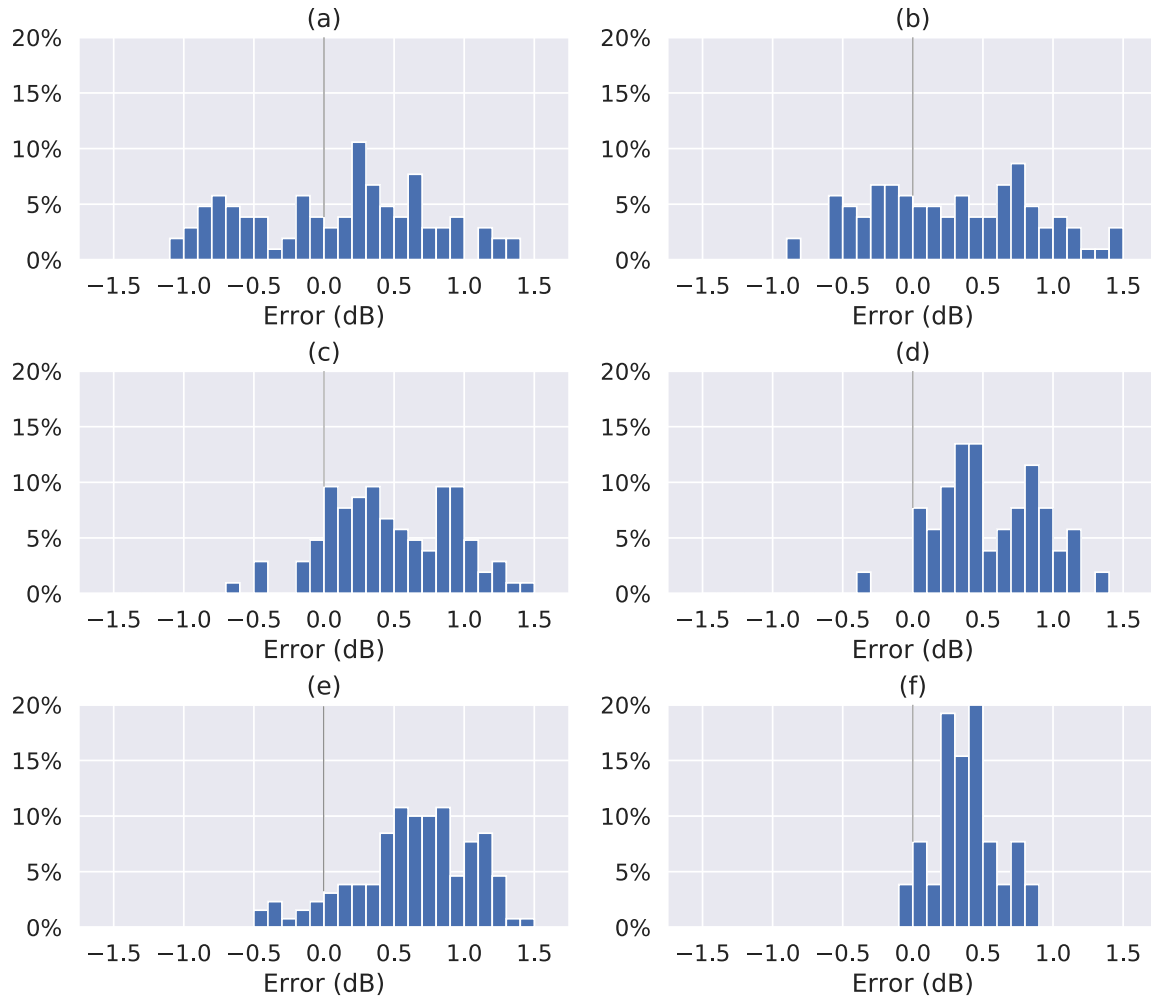


Fig. 4. Error distribution for different reaches: 400 km (a), 800 km (b), 1200 km (c), 1600 km (d), 2000 km (e) and 4000 km (f).

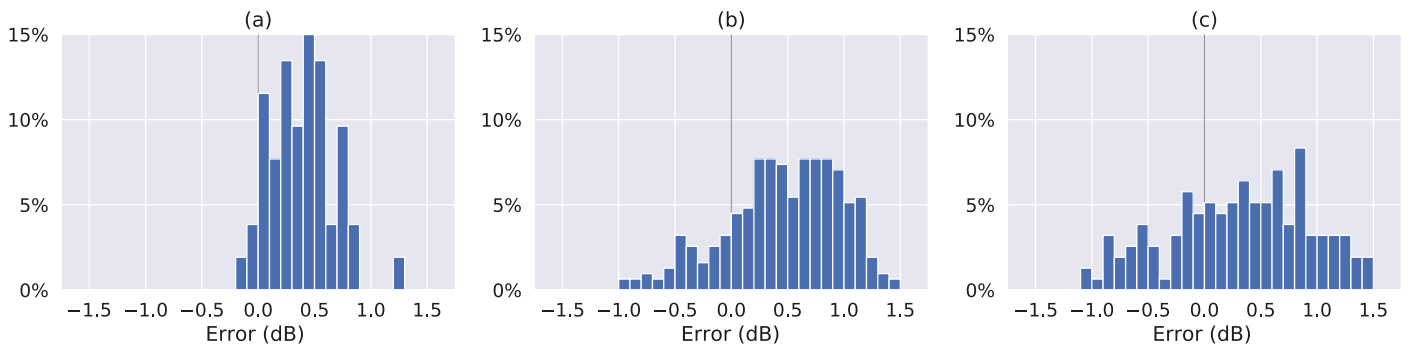


Fig. 5. Error distribution for different modulation formats: PM-QPSK (a), PM-8QAM (b) and PM-16QAM (c).

loss of 0.25 dB since it is the most conservative and we use this value for the rest of the analysis since it maximizes the conservatives of the estimations.

Once the connector loss is fixed equal to 0.25 dB, Figs. 4 report the error distribution for different reaches: 400 km (a), 800 km (b), 1200 km (c), 1600 km (d), 2000 km (e) and 4000 km (f). The cases of 400 km, 800 km and 1200 km are based on 100 samples each, then, the cases of 1600 km (d), 2000 km (e) and 4000 km are based on 50, 130 and 25 samples respectively. At 400 km, ~66% of the errors are conservative, the maximum error is 1.75 dB and 9% of the errors are above 1 dB. Then, at 800 km, the amount of conservative estimates grows up to 75%, while the largest error is still 1.75 dB and the 9% of the errors are larger than 1 dB. At 1200 km and 1600 km ~95% of the errors are positive, while, for both distances, the maximum error decreases to 1.5 dB and the percentage of errors above 1 dB decreases to 7%. Then, at 2000 km, 95% of the errors are conservative, the maximum error is 1.5 dB and 15% of them are larger than 1 dB. Finally, at 4000 km, almost all the errors are conservative and, being the maximum error 0.75 dB, all the errors are below 1 dB. In summary, the number of conservative errors grows with the distance, while the maximum error decreases. Except for the case at 2000 km, also the percentage of errors larger than 1 dB decreases with the distance. More in general, the error distribution narrows as the distance increases. This behaviour is due to the fact that the longer the distance, the higher the noise power, and this makes the estimation more accurate. Additionally, it is also more difficult to measure the GSNR for the shorter distances since the BER is smaller and therefore less statistically significant over a given time interval. Moreover, also the internal noise of the transceiver plays a role as it tends to hide the propagation noise when the latter is small, i.e. when the GSNR is high.

Figs. 5 report the error distribution for each modulation format: PM-QPSK (a), PM-8QAM (b) and PM-16QAM (c) over ~50, ~300 and ~150 samples respectively. The distribution of the PM-QPSK presents the smallest fluctuation being ~1 dB. Whereas, such a fluctuation increases to 2.5 dB for the other modulation formats. Moreover, the PM-QPSK presents the largest number of conservative and accurate errors since 97% of the errors are conservative, the largest error is 1.25 dB and 3% of the errors are conservative. For the PM-8QAM 88% of the errors are conservative, the maximum error is 1.75 dB and 9% of them is above 1 dB. Finally, for the PM-16QAM, 78% of the estimates are conservative, the maximum error is 1.75 dB and ~10% of the errors are larger than 1 dB. In general, the conservative capability and the accuracy decrease with the modulation format. This is due to the fact that PM-QPSK has been tested at the largest distances, where the fluctuations are smaller, while PM-16QAM has been probed at the shortest reaches of 400 km, 800 km and 1200 km. Consequently, we can say that, on average, the GSNR computation can reach higher accuracy for the smaller modulation formats when they cover the longer distances.

4. APPLICATION OF THE QOT COMPUTATION ON THE PRODUCTION NETWORK

In this section we describe the deployed network segments under analysis and we report the comparison between the QoT estimates with the measurements with the assumption of connector loss of 0.25 dB as derived from the analysis in the lab.

Table 4. Fiber parameters at 1550 nm.

Fiber type	α dB/km	D ps/nm/km	γ 1/W/km
NDSF	0.222	3.8	1.45
LS	0.24	4	1.41
ELEAF	0.2	4	1.41
TWRS	0.24	6	1.84

A. Network description

Figs. 6 show the topology of the two segments of the Microsoft core network under analysis. The first network segment, hereinafter called segment #1, is depicted in Fig. 6a. It is ~900 km long, and it has been loaded with 31 contiguous channels which propagate from one colorless mux/demux to the one on the other side. The second network segment (Fig. 6b), hereinafter called segment #2, reaches 1300 km carrying 26 contiguous channels along the entire network segment. In the segment #1, the span length varies from 30 km to 124 km, while in the segment #2 this value varies from 42 km to 88 km. The fiber types involved are NDSF and LS in the segment #1 and NDSF, ELEAF and TWRS fiber in the segment #2. The fiber parameters are reported in Table 4. Spans where including Raman amplifiers yield a net OSNR advantage feature hybrid Raman-EDFA amplifications, whereas others only contain EDFAs. Some intermediate ROADMs are placed between the edges in order to re-equalize the power. Each ROADM node is equipped with booster and pre-amplifier. The network has been configured for optimal performance by a vendor proprietary controller. The used optical band is between 191 THz and 192.6 THz for the segment #1 and between 191 THz and 192.36 THz with a 0.3 THz hole around 191.75 THz for the segment #2. The signals are root-raised cosine shaped, spaced 37.5 GHz and modulated with PM-8QAM modulation. The portions of spectrum not carrying data channels are filled with ASE in order to fully populate the line system.

For the connector losses we assume them to be equal to 0.25 dB. Despite it is expected that a production network presents larger connector losses, we have observed that smaller is the connector loss and more conservative are the results. Therefore, If the actual connector losses are larger we expect that this will mainly enlarge the errors in the positive direction.

B. Results

Figs. 7 report the measured GSNR values (triangular markers), the estimated GSNR provided by GNP_y (blue curve) and a ± 1 dB error bar (light blue band) both for the segment #1 (top) and the #2 (bottom) in forward (left column) and backward (right column) direction for a total of 114 values. GNP_y accurately captures the frequency dependent trend of GSNR. Moreover, most of the estimates are within 1 dB of error and conservative, with the estimates generally smaller than the measurements. Furthermore, one outlier can be noted at 191.0375 THz having very poor GSNR leading an error of -1.15 dB. This is likely caused by the transceiver not following the B2B characteristic rather than a propagation impairment since typically propagation disturbances do not exhibit such a strong frequency variation.

Fig. 8 reports the histogram (blue bars) and the cumulative distribution curve (orange curve) of the aggregated errors containing a total of 114 samples. The background is red for the

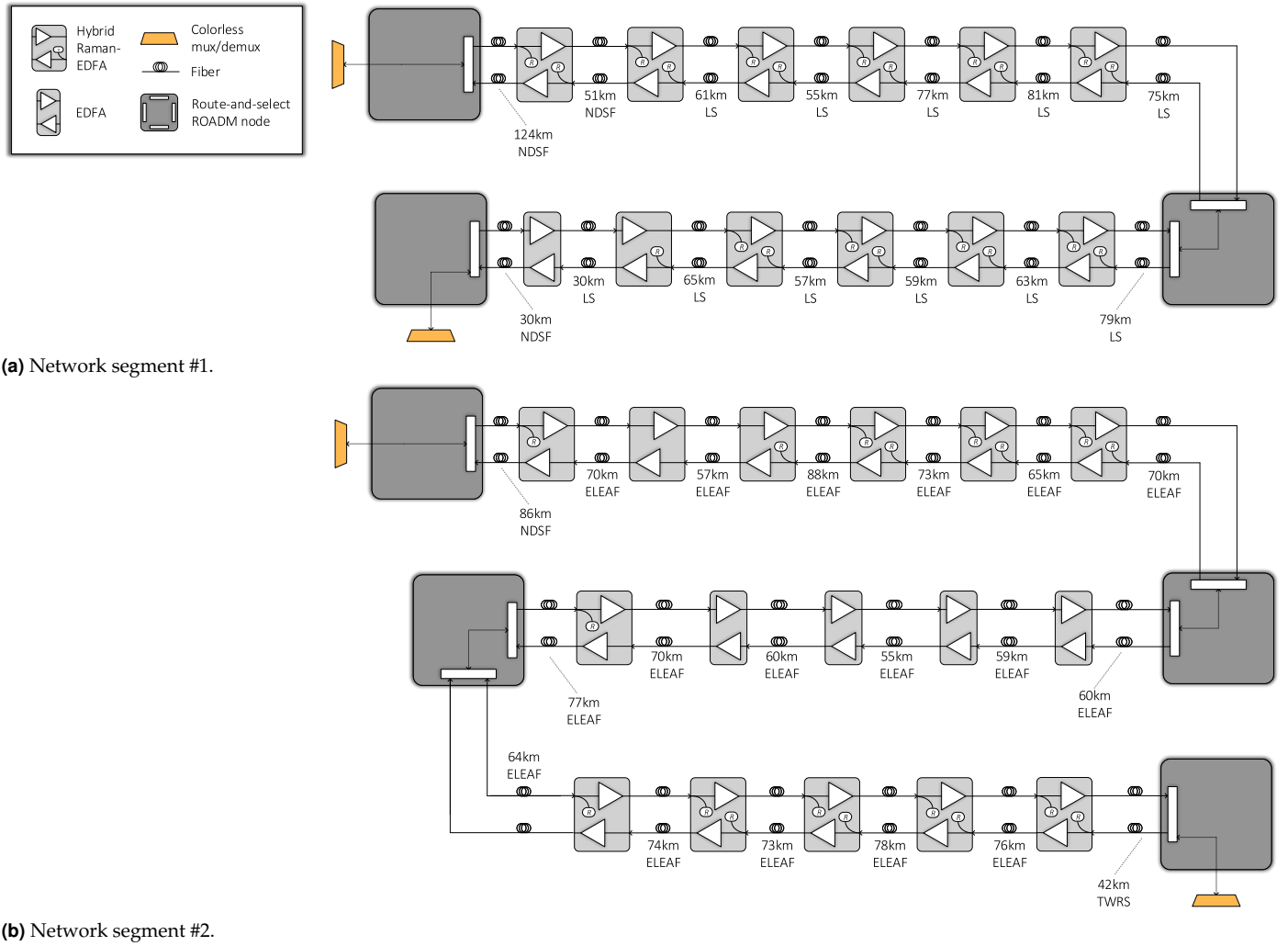


Fig. 6. Block scheme of the two segments of the Microsoft core network under analysis.

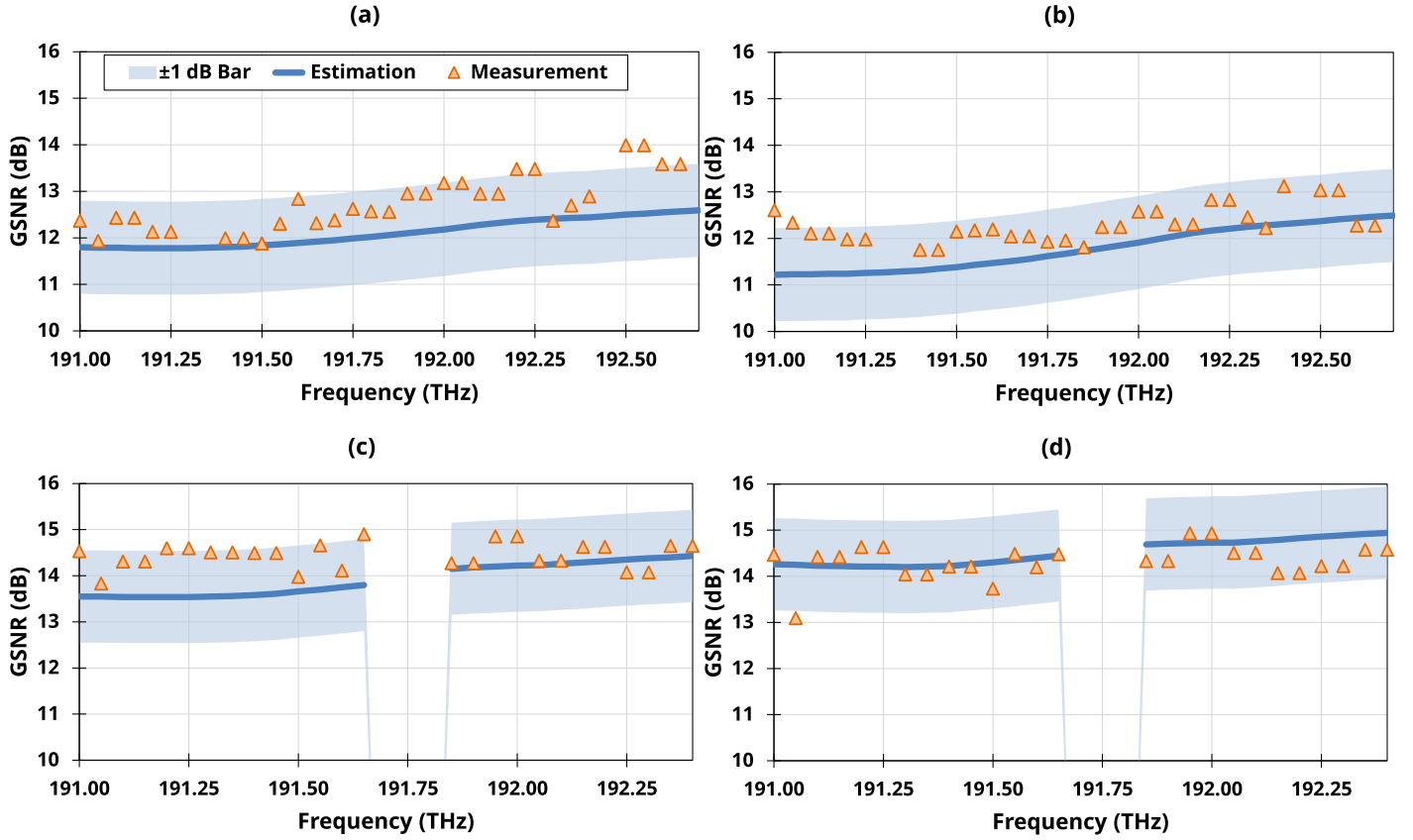


Fig. 7. Comparison between the estimated and the measured GSNR including a ± 1 dB bar for segment #1 both from A to Z (a) and vice-versa (b) and for segment #2 from A to Z (c) and vice-versa (d).

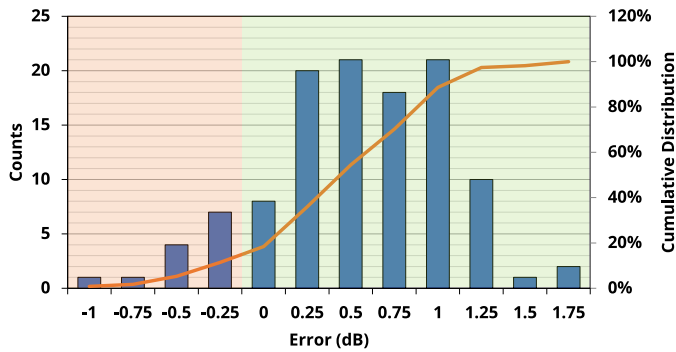


Fig. 8. Error histogram and cumulative distribution over all measured points.

negative errors (non conservative) and green for the positive ones (conservative). The largest error is +1.75 dB, while the most negative non-conservative error is -1.15 dB. Moreover $\sim 90\%$ of the errors are within ± 1 dB, while 95% of the estimates are conservative being greater than zero.

Summarizing, GNPpy provided accurate while conservative estimations of GSNR over a major cloud provider's deployed network, where non-ideal conditions such as aging of the components, sub-optimal connector cleanliness, and the presence of multiple splices along the fiber path play a key role and have the potential to affect the GSNR.

5. CONCLUSIONS

We have described the network abstraction of the physical layer by means of a weighted graph having the structure of the QoT-E of GNPpy. Then, we described the methodology adopted to obtain the measured GSNR, including the network performance metrics needed to run GNPpy, in order to produce an estimate of GSNR. Such a methodology relies only on the information present in the documentation and on the data provided by the network equipment and therefore, the process can be fully automated. Subsequently, we assessed the impact of the connector loss uncertainties on the error distribution of the GSNR computations over an experiment carried out in the Microsoft lab over a 6-node commercial network by varying the value of the connector losses from 0.25 dB to 0.75 dB. We covered distances from 400 km up to 4000 km, and three different modulation formats: PM-QPSK, PM-8QAM and PM-16QAM. The outcomes show an increase in the accuracy and in the number of conservative estimates with the increase in the reach and, in general, an accurate and conservative capability in estimating the GSNR as, only 90% of the errors are below ± 1 dB and 90% of them are conservative. Moreover, the QoT-E provides lower GSNR estimates for smaller connector losses since it tends to overestimate the NLI. Therefore, since the GSNR computation must be conservative other than accurate, a connector loss of 0.25 dB represents the best option.

Then, we use GNPpy with the assumption of connector loss of 0.25 dB to compute the GSNR on two network segments of the Microsoft production network. We demonstrated the efficacy

of this approach on two of Microsoft's live production routes as 90% of the estimates have an error within ± 1 dB and 95% of them are conservative.

ACKNOWLEDGMENTS

GNPy is an output of the Open Optical & Packet Transport (OOPT) - Physical Simulation Environment (PSE) group of the Telecom Infra Project [5].

REFERENCES

1. OIF, "Implementation Agreement 400ZR," https://www.oiforum.com/wp-content/uploads/OIF-400ZR-01.0_reduced2.pdf.
2. "COBO," <https://www.onboardoptics.org/>. Accessed: 2020-07-01.
3. OpenConfig, "Vendor-neutral, model-driven network management designed by users," <http://openconfig.net/>.
4. M. Birk, O. Renais, G. Lambert, C. Betoule, G. Thouenon, A. Triki, D. Bhardwaj, S. Vachhani, N. Padi, and S. Tse, "The openroadm initiative," *IEEE/OSA J. Opt. Commun. Netw.* **12**, C58–C67 (2020).
5. "TIP Open Optical & Packet Transport (OOPT)," <https://telecominfraproject.com/oopt/>.
6. A. Ferrari, M. Filer, K. Balasubramanian, Y. Yin, E. Le Rouzic, J. Kundrát, G. Grammel, G. Galimberti, and V. Curri, "Gnpy: an open source application for physical layer aware open optical networks," *J. Opt. Commun. Netw.* **12**, C31–C40 (2020).
7. J. Kundrát, E. L. Rouzic, James, J.-L. Augé, A. Ferrari, J. Mårtensson, G. Goldfarb, G. Grammel, M. Cantono, Robert, M. Garrich, A. D'Amico, B. Taylor, D. Boertjes, M. Naser, S. Z. (Troy), X. Liu, and D. Landa, "Telecominfraproject/oopt-gnpy: Optical Route Planning Library, Based on a Gaussian Noise Model," DOI:10.5281/zenodo.3458319 (2020).
8. "OOPT-GNPy web app," <https://gnpy.app/>. Accessed: 2020-07-01.
9. B. D. Taylor, G. Goldfarb, S. Bandyopadhyay, V. Curri, and H.-J. Schmidtko, "Towards a route planning tool for open optical networks in the telecom infrastructure project," in *Optical Fiber Communication Conference*, (Optical Society of America, 2018), pp. Tu3E–4.
10. M. Filer, M. Cantono, A. Ferrari, G. Grammel, G. Galimberti, and V. Curri, "Multi-vendor experimental validation of an open source QoT estimator for optical networks," *J. Light. Technol.* **36**, 3073–3082 (2018).
11. A. Ferrari, M. Filer, K. Balasubramanian, Y. Yin, E. Le Rouzic, J. Kundrát, G. Grammel, G. Galimberti, and V. Curri, "Experimental validation of an open source quality of transmission estimator for open optical networks," in *2020 Optical Fiber Communications Conference and Exhibition (OFC)*, (IEEE, 2020), pp. 1–3.
12. M. Filer, J. Gaudette, Y. Yin, D. Billor, Z. Bakhtiari, and J. L. Cox, "Low-margin optical networking at cloud scale," *IEEE/OSA J. Opt. Commun. Netw.* **11**, C94–C108 (2019).
13. V. Kamalov, M. Cantono, V. Vusirikala, L. Jovanovski, M. Salsi, A. Pilipetskii, D. K. M. Bolshtyansky, G. Mohs, E. R. Hartling, and S. Grubb, "The subsea fiber as a Shannon channel," in *In Proceedings of the SubOptic*, (2019).
14. V. Curri, "Software-defined WDM optical transport in disaggregated open optical networks," in *2020 22nd International Conference on Transparent Optical Networks (ICTON)*, (2020), pp. 1–4.
15. F. Zhang, Q. Zhuge, and D. V. Plant, "Fast analytical evaluation of fiber nonlinear noise variance in mesh optical networks," *IEEE/OSA J. Opt. Commun. Netw.* **9**, C88–C97 (2017).
16. M. Cantono, D. Pileri, A. Ferrari, C. Catanese, J. Thouras, J.-L. Augé, and V. Curri, "On the interplay of nonlinear interference generation with stimulated Raman scattering for QoT estimation," *J. Light. Technol.* **36**, 3131–3141 (2018).
17. I. Roberts, J. M. Kahn, J. Harley, and D. W. Boertjes, "Channel Power Optimization of WDM Systems Following Gaussian Noise Nonlinearity Model in Presence of Stimulated Raman Scattering," *J. Light. Technol.* **35**, 5237–5249 (2017).
18. D. Semrau, R. I. Killey, and P. Bayvel, "The Gaussian noise model in the presence of inter-channel stimulated raman scattering," *J. Light. Technol.* **36**, 3046–3055 (2018).
19. J. Kundrát, A. Campanella, E. Le Rouzic, A. Ferrari, O. Havliš, M. Hažlinský, G. Grammel, G. Galimberti, and V. Curri, "Physical-layer awareness: Gnpy and onos for end-to-end circuits in disaggregated networks," in *Optical Fiber Communication Conference*, (Optical Society of America, 2020), pp. M3Z–17.
20. J. Kundrát, O. Havliš, J. Jedliňský, and J. Vojtěch, "Opening up ROADMs: Let us build a disaggregated open optical line system," *J. Light. Technol.* **37**, 4041–4051 (2019).
21. J. Kundrát, O. Havliš, J. Radil, J. Jedliňský, and J. Vojtěch, "Opening up roadms: a filterless add/drop module for coherent-detection signals," *J. Opt. Commun. Netw.* **12**, C41–C49 (2020).
22. "Exchange with GNPy to check path feasibility," <https://git.opendaylight.org/gerrit/c/transportpce/+81785>.
23. E. Mateo, K. Nakamura, T. Inoue, Y. Inada, and T. Ogata, "Nonlinear characterization of fiber optic submarine cables," in *2017 European Conference on Optical Communication (ECOC)*, (IEEE, 2017), pp. 1–3.
24. "Characteristics of a single-mode optical fibre and cable," <http://handle.itu.int/11.1002/1000/10389>.
25. D. J. Elson, G. Saavedra, K. Shi, D. Semrau, L. Galdino, R. Killey, B. C. Thomsen, and P. Bayvel, "Investigation of bandwidth loading in optical fibre transmission using amplified spontaneous emission noise," *Opt. express* **25**, 19529–19537 (2017).
26. R. T. Fielding and R. N. Taylor, *Architectural styles and the design of network-based software architectures*, vol. 7 (University of California, Irvine Doctoral dissertation, 2000).